Optimal Solenoidal Interpolation of Turbulent Vectors: Application to PTV and Super-resolution PIV

Prakash Vedula[(1)] and R. J. Adrian[(2)]

Department of Theoretical and Applied Mechanics

University of Illinois, Urbana, Illinois 61801

[(1)]E-Mail: pvedula@uiuc.edu

[(2)]E-Mail: rjadrian@uiuc.edu

ABSTRACT

A new approach for the interpolation of a filtered turbulence velocity field given random point samples of unfiltered turbulence velocity data is described. In this optimal interpolation method, the best possible value of the interpolated filtered field is obtained as a stochastic estimate of a conditional average, which minimizes the mean square error between the interpolated filtered velocity field and the true filtered velocity field. Besides its origins in approximation theory, the optimal interpolation method also has other advantages over more commonly used *ad hoc* interpolation methods (like the 'adaptive Gaussian window'). The optimal estimate of the filtered velocity field can be guaranteed to preserve the solenoidal nature of the filtered velocity field and also the underlying correlation structure of both the filtered and the unfiltered velocity fields. The *a posteriori* performance of the optimal interpolation method is evaluated using data obtained from high-resolution direct numerical simulation of isotropic turbulence. Our results show that for a given sample data density, there exists an optimal choice of the characteristic width of cut-off filter that gives the least possible relative mean square error between the true filtered velocity and the interpolated filtered velocity. The width of this 'optimal' filter and the corresponding minimum relative error appear to decrease with increase in sample data density. The errors due to the optimal interpolation method are observed to be quite low for appropriate choices of the data density and the characteristic width of the filter. The optimal interpolation method is also seen to outperform the 'adaptive Gaussian window', in representing the interpolated field given the data at random sample locations. The overall *a posteriori* performance of the optimal interpolation method was found to be quite good and hence makes a potential candidate for use in interpolation of PTV and super-resolution PIV data.

1. INTRODUCTION

Particle tracking velocimetry (PTV) measures the velocities of sparse, individual particles located at random points in the flow; super-resolution particle image velocimetry (PIV) (Keane, Adrian and Zhang, 1995) achieves the same type of measurements in higher concentrations of particles by first estimating the vector field with a multi-particle correlation algorithm. In each case, an important post-processing step is the interpolation of the random point samples of the velocity vector field onto a uniform grid, or onto a continuous function. Interpolation of randomly sampled, random data is interesting because it is not subject to the requirements of Nyquist's criterion, but it may introduce significant distortion of the signal (Adrian and Yao, 1987, Mueller, Nobach and Tropea, 1998, Benedict, Nobach and Tropea, 2000). Discontinuities in the interpolating function can introduce wide-band noise, and missing information about the small-scale fluctuations between interpolating points leads to attenuation of the measured spectrum.

Perhaps the most common method for interpolating PTV data is the 'adaptive Gaussian window' or AGW (Koga, 1986, Agui and Jimenez, 1987, Spedding and Rignot, 1993). Letting $\mathbf{v}_p$ denote the velocity of the particle '*p*' that resides at $\mathbf{x}_p$ at time t, and $\mathbf{u}(\mathbf{x},t)$ denote the Eulerian velocity field, the velocity of a particle that follows the fluid motion with negligible slip is equal to a random point sample of the Eulerian field,

$$\mathbf{u}(\mathbf{x}_p,t) = \mathbf{v}_p(t). \tag{1}$$

The AGW algorithm uses the set of samples $\{\mathbf{u}_p\}$ contained in a spatial window $W(\mathbf{x})$ to form the interpolated field

$$\bar{\mathbf{u}}(\mathbf{x},t) = \frac{\sum_{\{\mathbf{x}_p\}\in W(\mathbf{x})} \mathbf{u}_p(\mathbf{x}_p,t) G(\mathbf{x}_p - \mathbf{x})}{\sum_{\{\mathbf{x}_p\}\in W(\mathbf{x})} G(\mathbf{x}_p - \mathbf{x})}, \tag{2}$$

where G(**x**) is typically a Gaussian function. (By letting G be a second order tensor, one can form the interpolation in such a way that the interpolated field is solenoidal, c.f. Zhong, *et al*., 1991.) Since G vanishes for large distances from x, the summations can be extended over the entire space of particles; restricting the summations to the window is just a computational convenience. Some insight is gained by expressing (2) in terms of the random point sample function

$$g(x,t) = \sum_{\forall p} d(x - \mathbf{x}_p). \tag{3}$$

The interpolated field can be expressed as,

$$\bar{\mathbf{u}}(\mathbf{x},t) = \frac{\int \mathbf{u}(x,t) G(x - \mathbf{x}) g(x,t) dx}{\int G(x - \mathbf{x}) g(x,t) dx}, \tag{4}$$

from which one sees that the interpolated field is linear in u, but decidedly non-linear in the random locations of the samples. This causes a problem in interpreting $\bar{\mathbf{u}}$: it cannot be expressed simply as a filtered form of the Eulerian field, u, due to the appearance of g and x in both the numerator and the denominator. If we tried to write $\bar{\mathbf{u}}$ as a convolution with a filter response function, (4) implies that the impulse response would depend upon g, i.e. the filter would be a random function of the random particle positions. A second issue with the AGW and similar variations is simply that it is *ad hoc*. This is common to most interpolation schemes, but unsatisfying, never the less. Owing to the *ad hoc* nature of these interpolation methods, the interpolated field is also not guaranteed to have the same dynamical structure as the underlying field.

In order to address these limitations, we consider an 'optimal' interpolator on the mathematical basis that it is required to yield the least mean square error function of either the velocity field or the filtered velocity field. Recognizing that we may not fully recover the random field from random samples, let us generalize our efforts to estimating a filtered version of the Eulerian field,

$$\tilde{u}_i(\mathbf{x},t) = \int h_{ij}(x,\mathbf{x})\, u_j(x,t)\, dx \tag{5}$$

(This form allows for inhomogeneous filters that depend explicitly on x. To preserve the solenoidal property of the filtered field, it is necessary to introduce a second order tensor for the filter impulse response, h_{ij}. Then, it is possible to construct the impulse response so that $\partial\tilde{u}_i / \partial x_i = \int \partial h_{ij}(x,\mathbf{x}) / \partial x_i \; u_j(x,t)\, dx = 0$.) Given the data $\{\mathbf{x}_p\},\{\mathbf{u}_p\}$ we seek to determine an estimator $\breve{\tilde{\mathbf{u}}}$ that represents each component of the filtered vector field with least mean square error:

$$e_i = \left\langle \left(\breve{\tilde{u}}_i - \tilde{u}_i\right) \middle| \{\mathbf{u}_p\},\{\mathbf{x}_p\} \right\rangle, \qquad \mathrm{i} = 1,2,3. \tag{6}$$

The exact solution to this minimization problem can be shown to be

$$\breve{\tilde{u}}_i(\mathbf{x},t) = \left\langle \tilde{u}_i(\mathbf{x},t) \middle| \{\mathbf{u}_p\},\{\mathbf{x}_p\} \right\rangle, \tag{7}$$

the conditional average of the turbulent velocity field given the values of the random velocity samples and the points at which they were measured (c.f. Papoulis, 1984, Adrian, 1996). Equation (7) averages over all possible velocity fields that are consistent with the measured data. Note that (7) is linear in u, but it may be non-linear in both the position data and the velocity data.

Direct use of the exact solution given by (7) is infeasible because the space of velocity-position data is huge. A typical two-dimensional PTV experiment might have of order 10^4 two-dimensional velocity samples corresponding to a 10^8 dimensional function. As in the optimal algorithm numerical method of Adrian (1977) for the turbulent Navier-Stokes equations, practical implementation of the optimal method requires approximation. The linear stochastic estimate of the conditional average in (7) is found by expanding the conditional average as a power series in the velocity data and truncating at first order:

$$\hat{\breve{\tilde{u}}}_i = linear\ \ estimate\ \left\langle \tilde{u}_i(\mathbf{x},t) \middle| \{\mathbf{u}_p\},\{\mathbf{x}_p\} \right\rangle = A_i(\mathbf{x},\{\mathbf{x}_p\}) + \sum_p B_{pij}(\mathbf{x},\{\mathbf{x}_p\})\, u_{pj}. \tag{8}$$

Substituting (8) into

$$e_i = \left\langle \left(\hat{\breve{\tilde{u}}}_i - \tilde{u}_i\right)^2 \middle| \{\mathbf{u}_p\},\{\mathbf{x}_p\} \right\rangle, \qquad \mathrm{i} = 1,2,3 \; e_i = \left\langle \left(\hat{\tilde{u}}_i - \tilde{u}_i\right)^2 \middle| \{\mathbf{x}_p\} \right\rangle, \qquad i = 1,2,3 \tag{9}$$

and minimizing with respect to variations of A_i and B_{pij}, one finds, after some manipulation,

$$\hat{\tilde{u}}_i = \left\langle \tilde{u}_i \right\rangle + \sum_p B_{pij}\left(u_{pj} - \left\langle u_{pj} \right\rangle\right), \tag{10}$$

where B_{pij} is found by solving the system of linear equations

$$\sum_p B_{pij} \left\langle u'_{pj} u'_{qj} \right\rangle = \left\langle \tilde{u}'_i u'_{qk} \right\rangle. \tag{11}$$

Here a prime denotes fluctuation with respect to the mean

$$(\cdot)' = (\cdot) - \langle(\cdot)\rangle. \tag{12}$$

The linear stochastic estimate has been shown to be quite good for various types of conditional averages of turbulence flows (Adrian, *et al.,* 1989).

Implementing (11) and (12) requires data input for $\langle u_i \rangle, \langle \tilde{u}_i \rangle, \langle u'_{pj} u'_{qk} \rangle, \langle \tilde{u}' u'_{qk} \rangle$. The mean of the unfiltered field can be found from the ensemble of experimental flow fields, provided that the number of samples is large enough to give a good average over a small area around the point in question. The maximum size of this area depends upon the rate at which the mean varies in space, but clearly its dimension can be at least as great as the displacement of the particles in the image fields. The mean of the filtered field can be found by filtering the mean field, since filtering and averaging commute.

The two-point spatial correlations between the velocity samples and the velocity sample and the velocity at the arbitrary location x can be approximated by assuming that the spatial separations lie in a range of distances corresponding to the inertial sub-range. The correlations may be modeled using correlations derived from the isotropic viscous-inertial turbulence spectrum, as an approximation to the true spectrum of the flow. While this approximation is not always justified, either because of insufficiently large Reynolds number or strong inhomogeneity and/or anisotropy, the interpolating functions still have the virtue of being rooted in fluid dynamics, and consequently they are less *ad hoc* than those used in other methods. The physics of high wave-number turbulence is imbedded in the process that determines the interpolating functions. The standard form of the isotropic representation only requires the longitudinal two-point correlation as input, and it guarantees that the correlation tensor is solenoidal, (Batchelor, 1960). It can be shown that the optimally interpolated field given by (10) is then also solenoidal.

These attractive features of optimal interpolation may not, however, guarantee better interpolation results. To judge this aspect one must appeal to *a posteriori* analysis of the optimal interpolation method. In this paper, we analyze the performance of the optimal interpolation method using random point samples of data, obtained from a high-resolution direct numerical simulation (DNS) of turbulence (with micro-scale Reynolds number, R_l ~164), that mimic PTV and super-resolution PIV results.

SIMULATION AND ERROR ANALYSIS

In order to test the *a posteriori* performance of the optimal interpolator, we consider known turbulence fields, where the statistics of filtered and unfiltered velocities can be accurately determined (except for sampling errors). This enables us to provide accurate inputs, for the two-point correlations, needed for obtaining a linear stochastic estimate of the 'optimal' interpolator, thereby eliminating *a priori* errors. The turbulence fields used in the present analysis are obtained using a well-resolved 256^3 numerical simulation of incompressible, forced isotropic turbulence (R_l ~164). Negative viscosity forcing on modes with wavenumber magnitude $k \leq 3$ was used to attain stationarity in time. The simulation is based on a pseudo-spectral algorithm (Rogallo 1981) and the time integration is done using a second-order Runga-Kutta method. The magnitudes of the minimum and maximum resolved wavenumbers are k=1 and k=121 respectively.

The effects of filtering are analyzed using a sharp Fourier cut-off filter, whose effect is to annihilate all Fourier modes of $|\mathbf{k}|$ greater than a cut-off wavenumber k_c and leave the rest of the modes unaltered. For each k_c, we associate a characteristic filter width $\Delta_c \equiv p / k_c$. The transfer function of this filter is $H(k_c - |\mathbf{k}|)$, where H denotes the Heaviside function. It can be shown that the filtered velocity field (5) obtained using this filter is solenoidal.

To obtain an estimate of a component of the filtered velocity field at any chosen point, given the three-dimensional vector information of velocities at *N* random points uniformly distributed over the entire cubic domain of side *L*, we need to solve *3N* equations (11). For high concentrations, the number of equations to be solved is very large and the linear system may include a number of equations that contribute little to the estimate owing to loss of correlation between the estimate and events for very large separations. This problem is addressed by dividing the entire cubic domain (with side *L*) into non-overlapping cubic sub-domains, each with side L_s (< *L*), and considering *M* (<< *N*) random samples that are uniformly distributed within each sub-domain. For each grid point location within a sub-domain, the estimate is evaluated based only on the events (or velocity samples) within that sub-domain and hence requires fewer equations (*3M*) to solve. The length L_s characterizes the maximum allowable loss of (longitudinal or transverse) correlation between the estimate and the event-data. It may also be useful to think of the role of L_s as that of an additional cut-off filter.

Given our choice of the filter (i.e. the Fourier cut-off filter), the performance of our optimal interpolator (10) for filtered velocities depends, *a priori*, on the following non-dimensional parameters: (i) L_s / l , (ii) $y \equiv M l^3 / L_s^3$ and (iii) Δ_c / l , where l denotes the Taylor micro-scale of the unfiltered velocity field and y represents the (normalized) data density. Hence, the normalized mean square error, $f \equiv e / s_{\tilde{u}}^2$, may be expressed as: $f = f(L_s / l , y , \Delta_c / l)$, where *e* denotes the component averaged mean square error between the true filtered velocity and the interpolated velocity and $s_{\tilde{u}}^2$ denotes the variance of the filtered velocity field.

The true filtered velocity at each of the (256^3) grid points in our computational domain can be obtained by the use of the transfer function on the true unfiltered velocity field. The evaluation of the interpolated filtered velocity requires the knowledge of the true velocities (*i.e.* event data) at each of the random sample points, obtained from a uniform distribution. The true velocities at these randomly sampled points are computed using a spectral interpolation procedure. Besides satisfying the solenoidal constraint on the event data, the spectral interpolation procedure also ensures that there are no errors in the specification of event data.

The correlations among event data, appearing on the LHS of (11), are evaluated using longitudinal velocity correlations obtained from DNS, along with the use of constraints imposed by isotropy and incompressibility of the flow. The correlations $\langle \tilde{u}' u'_{qk} \rangle$, between filtered and unfiltered velocities, appearing on the RHS of (11), can be shown to be equal to $\langle \tilde{u}' \tilde{u}'_{qk} \rangle$, for the case of a Fourier cut-off filter. Similar to the unfiltered correlation tensor, the latter correlation can be evaluated from the longitudinal filtered velocity correlations obtained from DNS. For more general use of the optimal interpolation method, for a wide range of Reynolds numbers, we can use the three-dimensional model spectrum of Pope (2000) to derive all correlations appearing in (11).

4. RESULTS AND DISCUSSION

The basic simulation parameters of the turbulence field obtained from DNS (using 256^3 grid points) summarized in Table 1 (in arbitrary simulation units). Note that $k_{\max}$ (= 121) is the magnitude of the maximum resolved wavenumber in our DNS. The three-dimensional energy spectrum obtained from DNS is shown in figure 1, as function of the wavenumber magnitude. We investigate the effects of filtering on the performance of the optimal interpolation procedure, by considering sharp Fourier cut-off filters at wavenumber magnitudes k_c = 121, 64, 32, 16, 8, 4. The case with k_c = 121 (or greater) corresponds to DNS (i.e. unfiltered velocity field). The dashed lines in figure 1 show the cut-off filter locations, each of which may be associated with a normalized characteristic filter width Δ_c / l .

The correlation tensor that appears on the LHS of (11) can be derived from a unique scalar function, i.e. the longitudinal correlation of filtered velocities, which is dependent on the cut-off wave number k_c. Figures 2a and 2b show the dependence of the longitudinal and transverse correlation coefficients of filtered velocities on k_c and the

separation distance (normalized by the Kolmogorov length scale, η). The transverse correlation function can also be derived from the longitudinal function (and vice versa), for the case of incompressible, isotropic turbulence. The longitudinal correlation coefficient ($r^{\parallel}$) of filtered velocities increases with decrease in k_c (or increase in Δ_c). The magnitude of the transverse correlation coefficient ($r^{\perp}$) of filtered velocities also appears to increase with k_c, for both small and large separations. However, the trend with k_c is not very clear in the zero-crossing region (around r/η ~180-200).

Table 1: Basic simulation parameters. N_0 (grid size), L (domain size), R_l (micro-scale Reynolds number), $\langle \varepsilon \rangle$ (energy dissipation rate), ν (viscosity), σ_u^2 (velocity variance), Δ (grid spacing), η (Kolmogorov length scale), λ (Taylor micro-scale), L_{11} (longitudinal integral length scale) in arbitrary simulation units

N_0	256
L	2π
R_l	164
$\langle \varepsilon \rangle$	62.9
ν	6.667×10^{-3}
σ_u^2	27.4
Δ/η	2.963
λ/η	25.228
L_{11}/η	121.331
k_{max}	121

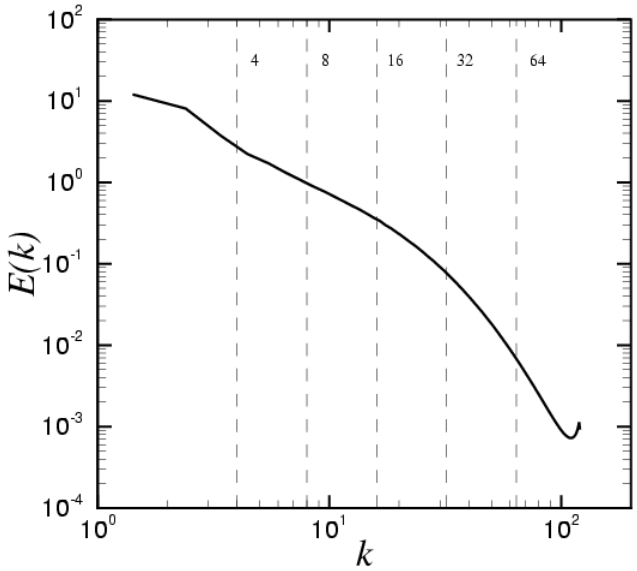

Figure 1: Three-dimensional energy spectrum E(k) versus k. The dashed lines denote the several cases of k_c used in our analysis

The amount of kinetic energy of filtered velocity field, relative to that of the unfiltered velocity field, for different k_c is shown in figure 3. The ratio of the variance of the filtered velocity field to that of the unfiltered velocity field decreases with increase in the characteristic width of the filter (or decrease in k_c). Besides being relevant to estimation equations (i.e. RHS of (11)), the variance of the filtered velocity field is also used in defining a normalized mean square error, f, due to the interpolation method.

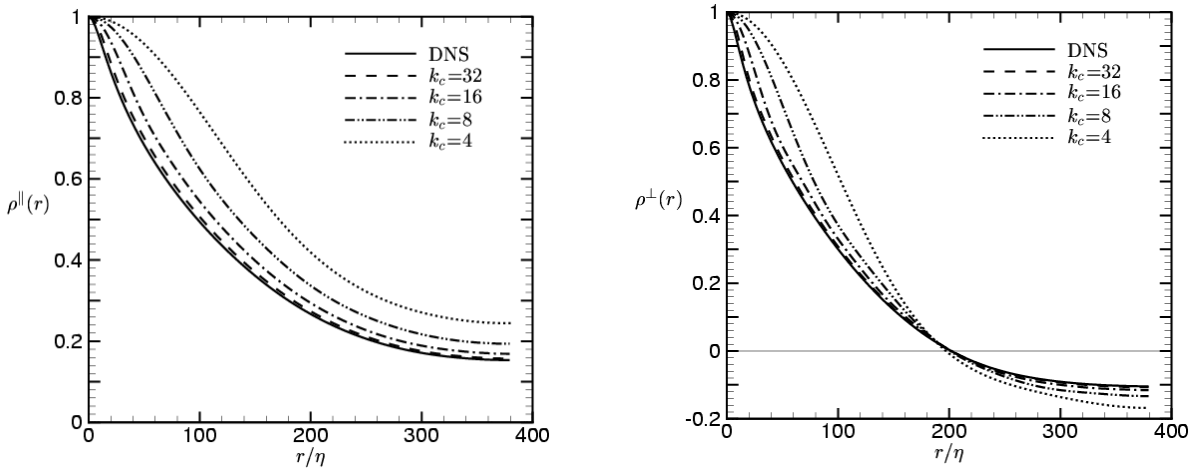

Figures 2a(left) and 2b(right): Longitudinal ($r^{\parallel}$) and transverse ($r^{\perp}$) correlation coefficients versus r/h for different k_c

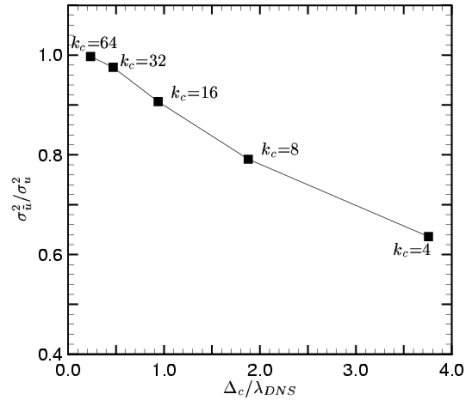

Figure 3: Ratio of the variances of unfiltered to filtered velocities versus the characteristic filter width relative to the Taylor micro-scale (of unfiltered velocity field).

The behavior of the normalized error f, which is a true indicator of the *a posteriori* performance of our optimal interpolation method, is shown in figures 4a, 4b and 4c. In figure 4a, the dependence of f on the (normalized) sample data density (y) and filter width is illustrated for a fixed L_s / l = 0.939. For any given y, the normalized mean square error f appears to have a minimum value (say $f_{\min}$). The value $f_{\min}$ and the width of the cut-off filter where $f_{\min}$ occurs are observed to decrease with increase in data density. Except for large bandwidth filters, the error f is also seen to decrease with increase in data density for any given width of the cut-off filter. The data points for the lowest Δ_c / l shown in figure 4a also represent the unfiltered DNS case. For the

highest data density case chosen, the minimum mean square error between the true filtered velocity and the velocity obtained from the optimal interpolation method is about 0.9% of the filtered velocity variance. For the lowest y chosen here (for L_s / l = 0.939), the minimum error is about 13.5% of the filtered velocity variance.

The mean square error obtained using the adaptive Gaussian window (AGW) is also shown in figure 4a (dashed line) for comparison. The high data density case with y = 77.184 was for chosen comparing the AGW method with our interpolation method. The performance of the optimal interpolation method appears to be much better than the AGW, with a relative error of only about 1% in the former case and about 11% in the latter.

Figures 4b and 4c represent cases with L_s / l fixed at twice and four times the value used in Figure 4a. The effects of moderate and low data densities are also illustrated in figures 4b and 4c respectively. The behavior of f and the trends with change in y are similar to the ones observed for figure 4a. The results from figures 4a-c suggest that our optimal interpolation method gives the best possible results for interpolating a filtered velocity field from a random sample of unfiltered velocities, if we appropriately choose the width of the cut-off filter. For very small filter widths, our optimal interpolation method gives better results with increase in filter cut-off width (for fixed L_s / l).

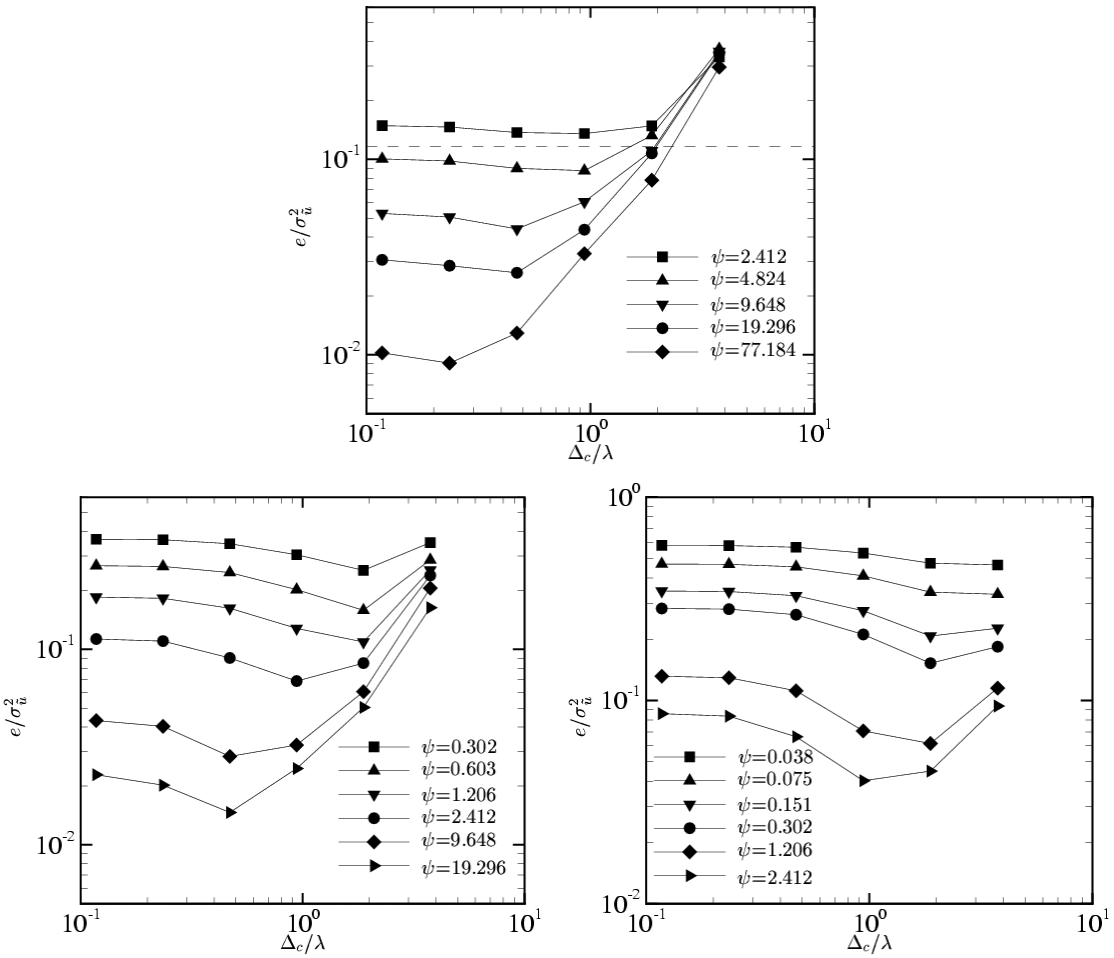

Figures 4a (top), 4b(bottom left) and 4c (bottom right): Normalized mean square error f versus normalized widths of the cut-off filters for several values of the normalized data density y . Figures 4a, 4b and 4c correspond to L_s / l = 0.939, 1.878 and 3.756 respectively. The dashed line in 4a shows the error due to AGW for y =77.184

The dependence of the error f on the data density y and L_s / l is better depicted in figure 5, which shows a plot of f versus y for different L_s / l. Two sets of curves shown here are for interpolation of (a) unfiltered velocity data and (b) filtered velocity data. For a given data density and filter width, the mean square error decreases with increase in L_s / l. The figure also suggests that for low data densities y and large L_s / l, optimal interpolation of a filtered velocity field yields a lower normalized error f compared to the interpolation of an unfiltered velocity field (for small widths of the cut-off filter). On the contrary, optimal interpolation of unfiltered velocity fields performs better than that of the filtered case for high data densities and low L_s / l.

A sample trace of the true filtered velocity signal along a line parallel to the x-axis is compared to the signal obtained from the optimal interpolation method, for (Δ_c / l ,y , L_s / l) = (0.470, 19.296, 1.878). We find that at the difference between the true filtered value and the value obtained from the optimal interpolation method, is small for most of the points on the chosen line. The relative mean square error f due to the optimal interpolation method is also low, about 1.5%, for the chosen parameter values.

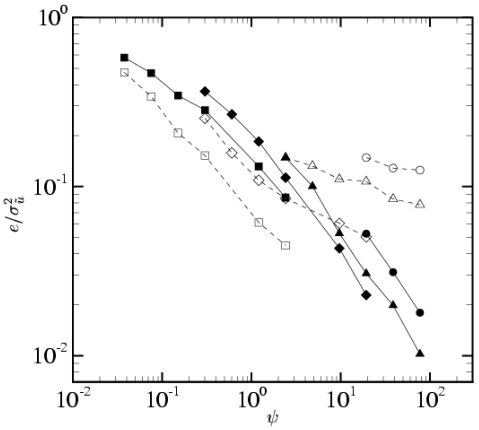

Figure 5: Normalized mean square error $f \equiv e / s_{\tilde{u}}^2$ versus normalized data density y . The solid lines correspond to the cases for unfiltered velocities where as the dashed lines correspond to those for the filtered field, with $k_c = 8$. The symbols viz. circles, triangles, diamonds and squares denote cases with L_s / l = 0.470, 0.939, 1.878 and 3.756 respectively

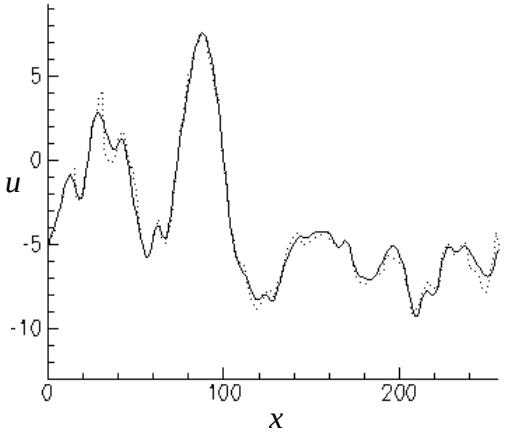

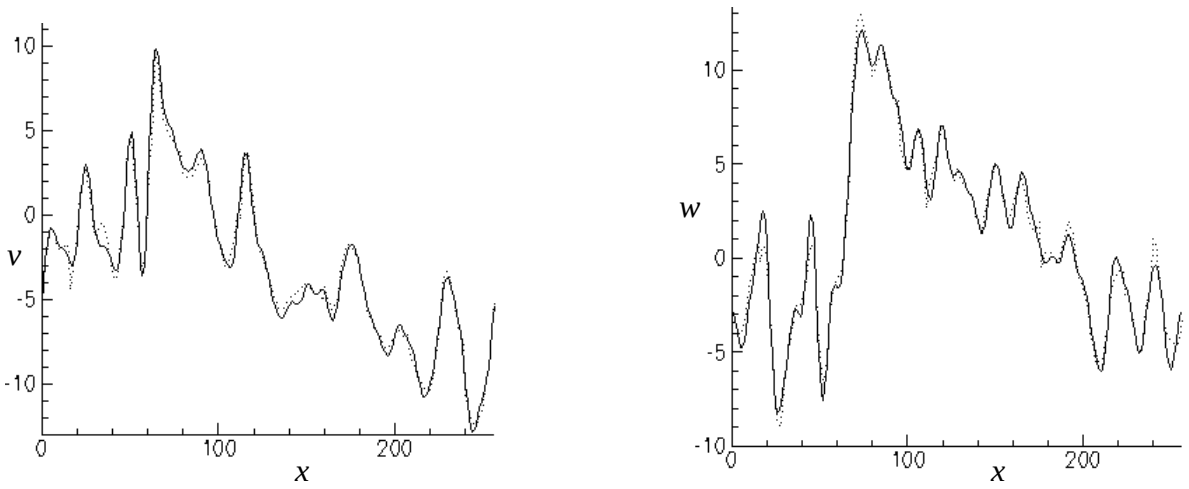

Figures 6: Instantaneous velocity components u, v and w along a line parallel to the x-axis. The solid and dotted lines denote the true filtered velocity signal and the interpolated signal obtained using optimal interpolation method

SUMMARY

The optimal interpolation process defines the best possible interpolator of the continuous turbulent velocity field given the available velocity data located at random points. Linear estimation of the conditional average is a method of proven accuracy in other contexts of turbulence representation, and application of the method to the interpolation problem yields a simple procedure that offers three attractive features: 1) the interpolated field is solenoidal; 2) the interpolation functions reflect approximate fluid dynamics of small scale turbulence; and 3) the interpolation allows for readily interpretable filtered field defined independently of the sampling process.

Our results indicate that there exists an optimal choice of the width of the cut-off filter that gives the least possible error in the interpolation of the filtered velocity field for any given density of the random point samples. For low data densities, optimal interpolation of the filtered velocities was found to be more reliable than the optimal interpolation of unfiltered velocities. In contrast to the *ad hoc* nature of AGW, the optimal interpolation method is based on a rational approach involving minimization of a mean square error function and this minimization is done by embedding the known statistical properties of the flow. These advantages are perhaps some of the reasons for the better *a posteriori* performance of the optimal interpolation method, compared to AGW. In the case of high Reynolds number flow experiments in a laboratory, the input correlations may be approximated using classical models of energy spectra. The sensitivity of the *a posteriori* performance of the optimal interpolation method to *a priori* errors in the approximation of these input correlations needs to be investigated further.

The optimal interpolation method appears to be a promising approach applicable for approximating filtered velocity field given the unfiltered velocities at random sample locations, obtained from PTV or super-resolution PIV. This approach may also be extended for interpolating other physical quantities of interest in turbulent flows such as filtered versions of velocity gradients, vorticity, scalar concentrations and scalar gradients given the relevant randomly spaced event data.

REFERENCES

Adrian, R. J. (1977). "On the role of conditional averages in turbulence theory," *Turbulence in Liquids*, Zakin and Patterson, eds., Science Press, Princeton, pp. 323-332

Adrian, R. J. and Yao, C. S. (1987). "Power spectra of fluid velocities measured by laser Doppler velocimetry," *Exp. Fluids*, 5, pp. 17-28

Adrian, R. J., Jones, B. G., Chung, M. K., Hassan, Y., Nithianandan, C. K. and Tung, A.T.-C. (1989). "Approximation of turbulent conditional averages by stochastic estimation," *Phys. Fluids A*, 1, pp. 992-998

Adrian, R. J. (1996). "Stochastic Estimation of the Structure of Turbulent Fields," In *Eddy Structure Identification*, Bonnet, J. P., ed., Springer: Berlin, pp. 145-196

Agui, J. and Jimenez, J. (1987). "On the performance of particle tracking velocimetry," *J. Fluid Mech*., 185, pp. 447-468

Batchelor, G. K. (1960). "*Homogeneous Turbulence*," Cambridge Univ. Press, New York

Benedict, L.H., Nobach, H. and Tropea, C. (2000). "Estimation of turbulent velocity spectra from laser Doppler data," *Meas. Sci. Tech*., 11, pp. 1089-1104

Keane, R. D., Adrian, R. J. and Zhang, Y. (1995). "Super-resolution particle-imaging velocimetry," *Meas. Sci. Tech*., 6, pp. 754-768

Koga, D. J. (1986). An interpolation scheme for randomly spaced sparse velocity data, *unpublished note*, Mech. Engr. Dept., Stanford Univ., Stanford, CA

Mueller, E., Nobach, H., Tropea, C. (1998). "Refined reconstruction-based correlation estimator for two-channel, non-coincidence laser Doppler anemometry," *Meas. Sci. Tech*., 9, 442-451

Papoulis, A. (1984). "*Probability, Random Variables and Stochastic Processes*," McGraw-Hill, New York

Pope, S. B. (2000). "*Turbulent flows*," Cambridge University Press, Cambridge

Rogallo, R. S. (1981) "Numerical experiments in homogeneous turbulence," Technical Report TM-81315, NASA Ames

Spedding, G. R. and Rignot, E. J. M. (1993). "Performance analysis and application of grid interpolation techniques for fluid flows," *Exp. Fluids*, 16, pp. 417-430

Zhong, J. L. (1995). "Vector-Valued Multidimensional Signal Processing and Analysis in the Context of Fluid Flows," *Ph.D. thesis*, University of Illinois

Zhong, J. L., Weng, J. Y. and Huang, T. S. (1991) "Vector field interpolation in fluid flow," *Digital Signal Processing '91*, Int'l. Conf. on DSP, Florence, Italy